BU-HEP 95-5
hep-ph/9502370
January 1995

Numerical investigations of baryon non-conserving processes in the electroweak theory *

Claudio Rebbi and Robert Singleton, Jr.

Physics Department

Boston University

590 Commonwealth Avenue

Boston, MA 02215, USA

* *Based on a lecture given by C. Rebbi at the 1994 ICTP Summer School in High Energy Physics and Cosmology, to be published in the proceedings of the School (World Scientific Publishing - Singapore - 1995).*

Abstract

We illustrate the use of computational methods for the study of baryon non-conservation in high energy electroweak processes.

1 Introduction

Since the advent of the modern scientific method, knowledge of the physical world has advanced through the interplay of experimental observation and theoretical analysis. Correspondingly, the terms experimental physics and theoretical physics have been used to characterize these two basic methodologies of scientific research.

The introduction of computers, however, has lead to the establishment of a third fundamental methodology and the term computational physics has been coined to denote all those investigations where computers are used in an intrinsic manner to unravel properties of complex systems. The methods of computational physics do not offer a replacement for either experimental investigation or theoretical analysis. Indeed, although computer modeling shares many of features of actual experiment, clearly the study of computer simulated phenomena can never replace the observation of the actual world. In a more subtle way, computational physics cannot displace theoretical physics either. The insights into the phenomena provided by the theoretical analysis constitute the necessary platform over which a computational investigation can be launched and are ultimately required to interpret the latter's results. Thus theoretical physics and computational physics complement each other and, at their best, proceed hand in hand.

Because of the large computer power required by some numerical investigations, it is frequently thought that computational physics is accessible only to a limited constituency of researchers fortunate enough to have access to powerful supercomputers. This belief is wrong, on two accounts. First, not all computational investigations require very large resources. In many instances, ingenuity more than powerful hardware is the key to a successful utilization of the computer. Second, the amazingly rapid pace of technological development in the field of computers is making these tools ever more accessible on a world wide scale. For these reasons, the International Center for Theoretical Physics has been offering colleges on computational physics on a rather regular basis since the first conference and college it held in 1986.

In particle physics some of the most successful computational applications have taken place in the area of lattice gauge theories, where computer simulations of quantum fluctuations have been used to evaluate several non-perturbative quantities of primary importance. In particular, computational investigations of QCD have provided evidence of quark confinement as well as the means of calculating hadronic observables such as meson and baryon masses, some weak matrix elements, the deconfining temperature and the value of α_S. However, the span of computational particle physics investigations is by no means limited to lattice QCD, and in these lectures we will illustrate another challenging application of numerical techniques to particle phenomena where computational and theoretical methods complement each other. We will see, indeed, that the theoretical analysis of the phenomenon provides the basis for the computational investigation, which in turn can produce information that goes well beyond the reach of purely analytic techniques.

The problem we will study is the possible occurrence of baryon number violation in high energy electroweak processes. In perturbation theory, baryon number is strictly conserved. But, as has been well known since the pioneering work of 't Hooft[1], the axial vector anomaly implies that baryon number is not conserved in processes which change the topology of the gauge fields. Baryon number violating amplitudes are non-perturbative, and viable methods of calculation are scarce. Basi-

cally there are two ways of getting at non-perturbative information in quantum field theory. One can use either semi-classical techniques or direct lattice simulations of the quantum fluctuations. Unfortunately, theories with small coupling constants are not suited for the latter, so the electroweak sector of the standard model lies beyond the reach of direct lattice calculations. This means that semiclassical methods presently offer the only way to study baryon number violating electroweak processes.

Electroweak baryon number violation is associated with topology change of the gauge fields. Classically, gauge field configurations with different topology (i.e differing by a topologically non-trivial gauge transformation) are separated by an energy barrier. The (unstable) solution of the classical equations of motion which lies at the top of the energy barrier is called the sphaleron[2]. At energies lower than the sphaleron energy, topology changing transitions, and hence baryon number violation, can only occur via quantum mechanical tunneling. Under certain circumstances, semiclassical methods can be used to approximate these tunneling rates. The relevant solution of the Euclidean equations of motion which describe such tunneling is known as the instanton[3].

All transitions that change topology involve fields of order $1/g$ and actions $S = S_0/g^2$, where S_0 is a coupling constant independent action reexpressed in terms of rescaled fields $gA_\mu(x)$. As a consequence, all tunneling amplitudes contain a barrier penetration factor $\exp(-S_0/g^2)$:

$$A \sim \exp(-S_0/g^2), \tag{1}$$

where S_0 is a numerical factor of order one. The appearance of the square of the electroweak coupling constant g in the denominator of the exponent in Eq. 1 has three important implications. First it tells us that the phenomenon is non-perturbative, in the sense that A has an essential singularity at $g = 0$ and thus cannot be expressed in terms of a perturbative expansion in powers of g. Second, the fact that the actual numerical value of g is very small indicates that non-perturbative semiclassical methods, based on saddle point expansions of path integrals around solutions of the classical equations of motion, are likely to produce reliable results (to better understand this point, remember that in units in which $\hbar$ is not set equal to 1, Eq. 1 takes the form $A \sim \exp[-S_0/(\hbar g^2)]$ so that small g and small $\hbar$ are equivalent). Third, the small value of g also makes these processes apparently irrelevant because the associated transition rates, proportional to $|A|^2$, turn out to be abysmally small.

This state of affairs changed a few years ago when Ringwald [4] and later Espinosa[5] noticed that a summation of the semiclassical amplitudes over final states gives rise to factors which increase very rapidly with increasing energy. This might lead to a compensation of the suppression factor in Eq. 1 for energies approaching the energy of the barrier, i.e. the sphaleron energy E_{sph}. Intuitively, one might expect the tunneling suppression factor to become much less severe as the energy approaches the energy of the barrier. In particular one might expect it to disappear altogether for $E > E_{sph}$, i.e. in the region where the topology changing processes are classically

allowed. Investigations have indeed confirmed that this is precisely what happens in high temperature electroweak processes[6] . As the temperature approaches E_{sph} the barrier-penetration suppression factor becomes progressively less pronounced, and electroweak baryon number violation becomes unsuppressed altogether for temperatures comparable to the sphaleron energy. The situation is, however, much less clear for high energy collisions. Phase space considerations are more subtle, and simply because one has enough energy to pass over the barrier does not guarantee that one does. The problem is that in high energy collisions the initial state is an exclusive two particle state, which is difficult to incorporate in a semiclassical treatment of the transition amplitude.

A possible remedy to this situation has recently been proposed by Rubakov, Son and Tinyakov[7], who suggested that one considers inclusive initial coherent states, but constrained so that energy and particle number take fixed average values

$$E = \frac{\epsilon}{g^2}, \tag{2}$$

$$N = \frac{\nu}{g^2}. \tag{3}$$

In the limit $g \to 0$, with ϵ and ν held fixed, the path integrals giving the transition amplitudes are then dominated by a saddle point configuration which solves the classical equations of motion. This permits a semiclassical calculation of the transition rates. Information on the high energy collision processes can then be obtained from the limit $\nu \to 0$. While this limit does not strictly reproduce the exclusive two-particle initial state, under some reasonable assumptions of continuity it can be argued that the corresponding transition rates will be equally suppressed or unsuppressed.

In these lectures we will not reproduce the derivation of the saddle point equations, which would form the topic of an extended set of lectures in itself. (Indeed, Rubakov presented such lectures at the 1992 ICTP Summer School in High Energy Physics and Cosmology, and the conversations that one of us held with him then stimulated the investigation we describe here.) Rather, we will start from these equations, which we will of course recapitulate, and describe the computational techniques used to solve them and the progress we have made in this direction. For the actual derivation of the equations the reader should consult Ref. [7].

In the next section we illustrate the general properties of topology changing evolution of the classical fields. For simplicity we first consider the 2-dimensional Abelian Higgs model. Then we examine the 4-dimensional $SU(2)$ Higgs model, but restricted to the spherical *Ansatz* to obtain a computationally tractable system. In Section 3 we investigate the properties of topology changing processes above the sphaleron barrier, i.e. in the classically allowed energy domain (see also Ref. [8]). And in Section 4 we finally describe the equations introduced by Rubakov, Son and Tinyakov[7] and the computational methods required to solve them.

2 Topology changing field evolution

The 1+1 dimensional Abelian Higgs system is defined in terms of a complex matter field $\phi(x)$ and an Abelian gauge potential $A_\mu(x)$ with action

$$S = \int dx^2 \ \left\{ -\frac{1}{4} F_{\mu\nu} F^{\mu\nu} + (D_\mu \phi)^* D^\mu \phi - \lambda (|\phi|^2 - 1)^2 \right\} \ , \tag{4}$$

where the indices run over 0 and 1, $F_{\mu\nu} = \partial_\mu A_\nu - \partial_\nu A_\mu$, $D_\mu \phi = \partial_\mu \phi - \imath A_\mu \phi$ and many inessential constants have been eliminated by a suitable choice of units.

The most important feature of this system is that the vacuum, i.e. the configuration of minimum energy, occurs for non-vanishing ϕ, indeed, with our special choice of units for $|\phi| = 1$. Since this does not specify the phase of ϕ, there is not a unique vacuum state, but rather multiple vacua. Still, because of gauge invariance one must be careful in regard to the physical significance of the phase of ϕ. A local variation of the phase of ϕ can always be undone by a suitable gauge transformation. And since gauge equivalent configurations must be considered physically indistinguishable, local variations of the phase of the matter field do not lead to different vacua. However, variations of the phase of ϕ by multiples of 2π (as the coordinate x^1 spans the entire spatial axis) cannot be undone by a local gauge transformation, and thus define topologically distinct vacuum states. These vacua differ by the global topological properties of the field configuration. The condition $|\phi| = 1$ restricts the values of the matter field to the unit circle (in the complex plane). If we demand that ϕ takes fixed identical values as $x^1 \to \pm\infty$ (a condition we later relax), then the number of times ϕ winds around the unit circle as x^1 spans the entire real axis is a topological invariant (the winding number) and characterizes different topologically inequivalent vacuum states.

Figures 1a-c illustrate three contours traced in the complex plane by the field variable $\phi(x^1)$ as the coordinate x^1 spans the entire space axis. Inequivalent vacuum configurations with winding numbers 0 and 1 respectively are depicted in Figs. 1a and 1c. In the contour of Fig. 1a the phase of ϕ stays fixed at zero as x^1 ranges between $-\infty$ and $+\infty$, whereas it goes once around the unit circle in Fig. 1c. Thus the corresponding vacuum configurations have winding number 0 and 1. The detailed variation of the phase is immaterial since it can always be changed locally by a gauge transformation. Thus, in Fig. 1a for example, as x varies from $-\infty$ to $+\infty$ the field does not have to stay fixed, but could wander continuously on the unit circle provided the net change in phase is zero. However, the configuration of Fig. 1a cannot be continuously deformed to that of Fig. 1c without leaving the manifold of zero energy configurations. Therefore, in an evolution between neighboring vacua the field configuration must pass over an energy barrier, as illustrated in Fig. 1b which singles out the configuration for which ϕ vanishes at a point, rendering its phase there undefined. Figures 1d-f add the additional perspective of spatial dependence for the field $\phi(x^1)$. Figures. 1a-c can be viewed as projections onto the complex plane orthogonal to the x^1 axis of the curves in Figs. 1d-e.

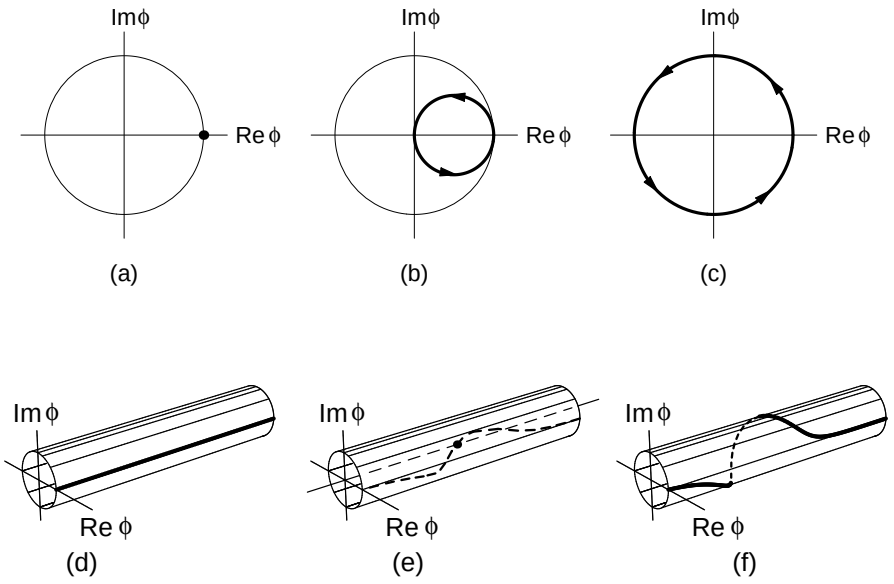

Figure 1: Example of two inequivalent vacuum configurations (a, c) and a field configuration at the top of the energy barrier separating them (b). Figures a, b and c trace the field ϕ in the complex plane as the spatial coordinate spans the entire axis. A three dimensional perspective has been added in figures d, e and f to illustrate the detailed dependence of ϕ on the spatial coordinate.

The condition that ϕ should take the same value at $x^1 = \pm\infty$ can be relaxed. Sometimes it is convenient to use the time independent gauge freedom to make $\phi(\infty)$ and $\phi(-\infty)$ differ (while keeping both fixed in time). Thus, the configurations of Figs. 1a-c can be gauge transformed into the configurations shown in Figs. 2a-c. In Fig. 2a the phase of ϕ changes by $-\pi$ as x^1 goes from $-\infty$ to $+\infty$, whereas in Fig. 2c it rotates by π. As in Fig. 1, the two vacuum configurations differ by a phase of 2π, i.e. by a unit change of winding number. In the intermediate configuration (Fig. 2b) the field takes only imaginary values. In this gauge the configuration which minimizes the energy on top of the barrier (i.e. the sphaleron configuration) takes a very simple form

$$\phi(x^1) = \imath \mathrm{th}[\sqrt{\lambda}(x^1 - c)], \quad A_\mu = 0. \tag{5}$$

A possible parameterization for the entire evolution illustrated in Fig. 2 can be conveniently written

$$\phi(x^1) = \imath \frac{1 - \exp[\imath\tau - 2\sqrt{\lambda}(x^1 - c)]}{1 + \exp[\imath\tau - 2\sqrt{\lambda}(x^1 - c)]}, \tag{6}$$

$$A_0 = 0, \quad A_1 = \frac{4\tau\sqrt{\lambda}}{\pi \mathrm{ch}[2\sqrt{\lambda}(x^1 - c)]}. \tag{7}$$

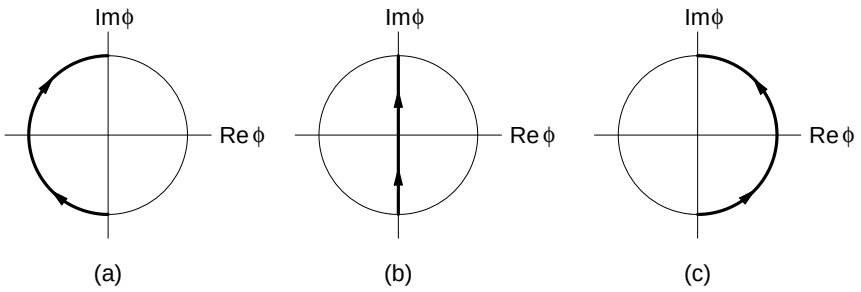

Figure 2: A different gauge equivalent representation of the configurations illustrated in Fig. 1.

As the reader can easily verify, for $\tau = -\pi/2$ and $\tau = \pi/2$ the field ϕ reduces to a number of unit modulus precisely spanning the contours of Fig. 2a and Fig. 2c respectively (as as x^1 ranges from $-\infty$ to $+\infty$). The corresponding values of A_1 are chosen to make the gauge covariant derivative of ϕ vanish, thus ensuring vacuum. We should point out, however, that Eqs. 6,7 do not represent the solution of any special equations of motion (Euclidean or Minkowski). They are merely a compact parameterization of interpolating configurations, in terms of two variables c and τ, which might be useful in studying sphaleron transitions based on the method of collective coordinates.

If one couples chiral fermions to the gauge field in the 2-dimensional Abelian Higgs model the fermionic current has an anomaly which leads to fermion number violation in the topology changing processes described above. Thus this model would appear a very convenient system for a simplified study of baryon number violation in high energy processes. However, as we will discuss in the next section, a crucial component of the computational investigation is the ability to numerically identify the normal mode amplitudes of the fields in the asymptotic regime. No matter how non-linear the system may be at any given point in its evolution, typically the energy will eventually disperse and bring the system to a regime where the fields undergo small oscillations about a vacuum configuration. This dispersion is expected to occur in any field theoretical system, unless prevented by conservation laws such as those underlying soliton phenomena. Now, while the 2-dimensional Abelian Higgs model does not possess soliton solutions, we have observed computationally that the decay of the sphaleron in this system nevertheless gives origin to persistent, localized, large oscillations with an extremely small damping rate (this observation was also made by Arnold and McLerran in Ref. [9]).These oscillations, illustrated in Fig. 3, make the system quite unwieldy for a computational investigation of baryon number violation based on semiclassical techniques. Thus we eventually turned our attention to the more realistic 4-dimensional $SU(2)$ Higgs system, which constitutes the most relevant component of the full electroweak theory. Because of the larger dimensionality of space one would expect the energy to disperse much more readily in this system, an expectation borne out by results of Hellmund and Kripfganz[10], who observed the

Figure 3: Sphaleron decay in the 2-dimensional Abelian Higgs model: evolution of the ϕ field. The values of the phase of the complex field are coded by shades of gray, and the modulus of the field by the height of the surface. The sphaleron decays rather quickly, but leaves behind a quasi-stable oscillating remnant.

onset of a linear regime following the sphaleron's decay.

The 3+1 dimensional $SU(2)$ Higgs system is defined in terms of a complex doublet $\Phi(x)$ and the gauge potential $A_\mu(x)$ with action

$$S = \int dx^4 \ \left\{ -\frac{1}{4} F_{\mu\nu} F^{\mu\nu} + (D_\mu \phi)^* D^\mu \Phi - \lambda (|\Phi|^2 - 1)^2 \right\} \ , \tag{8}$$

where the indices run over $0 \cdots 3$ and where

$$F_{\mu\nu} = \partial_\mu A_\nu - \partial_\nu A_\mu - \imath [A_\mu, A_\nu] \tag{9}$$

$$D_\mu \Phi = (\partial_\mu - \imath A_\mu) \Phi \tag{10}$$

with $A_\mu = A^a_\mu \sigma^a / 2$. We use the standard metric $\eta_{\mu\nu} = \mathrm{diag}(1, -1, -1, -1)$, and have eliminated many inessential constants by a suitable choice of units. We focus on the spherically symmetric configurations of Ratra and Yaffe[11], which reduce to an effective 2-dimensional theory. This lower dimensional theory has the full topological structure of the 4-dimensional system, while having the virtue of being computationally manageable.

The spherical *Ansatz* is given by expressing the gauge and Higgs fields in terms of six real functions a_0 , a_1 , α , β , μ and ν of r and t:

$$
\begin{aligned}
A_0(\mathbf{x},t) &= \frac{1}{2}\,a_0(r,t)\boldsymbol{\sigma}\cdot\hat{\mathbf{x}} \\
A_i(\mathbf{x},t) &= \frac{1}{2}\,[a_1(r,t)\boldsymbol{\sigma}\cdot\hat{\mathbf{x}}\hat{x}^i + \frac{\alpha(r,t)}{r}(\sigma^i - \boldsymbol{\sigma}\cdot\hat{\mathbf{x}}\hat{x}^i) + \frac{1+\beta(r,t)}{r}\epsilon^{ijk}\hat{x}^j\sigma^k] \\
\Phi(\mathbf{x},t) &= [\mu(r,t) + i\nu(r,t)\boldsymbol{\sigma}\cdot\hat{\mathbf{x}}]\xi\ , \qquad (11)
\end{aligned}
$$

where $\hat{\mathbf{x}}$ is the unit three-vector in the radial direction and ξ is an arbitrary two-component complex unit vector. Note that configurations in the spherical *Ansatz* remain in the spherical *Ansatz* under gauge transformations of the form

$$
\begin{aligned}
A_\mu &\quad \to A_\mu + \imath U^\dagger\partial_\mu U \qquad \mu = 0\cdots 3 \qquad (12)\\
\Phi &\quad \to U\Phi\ , \qquad (13)
\end{aligned}
$$

where the gauge function is given by

$$
U = \exp[\imath\Omega(r,t)\boldsymbol{\sigma}\cdot\hat{\mathbf{x}}/2]\ . \qquad (14)
$$

Inserting Eqs. 11 directly into Eq. 8, one obtains an effective 2-dimensional theory with action

$$
\begin{aligned}
S = 4\pi\int dt\int_0^\infty dr \quad & \Big[-\frac{1}{4}r^2 f^{\mu\nu}f_{\mu\nu} + (D^\mu\chi)^* D_\mu\chi + r^2 D^\mu\phi^* D_\mu\phi \\
& -\frac{1}{2r^2}\Big(\ |\chi|^2 - 1\Big)^2 - \frac{1}{2}(|\chi|^2+1)|\phi|^2 - \mathrm{Re}(i\chi^*\phi^2) \\
& -\lambda\, r^2\ \Big(|\phi|^2 - 1\Big)^2\ \Big]\ , \qquad (15)
\end{aligned}
$$

where the indices now run from 0 to 1 and in contrast to Ref. [11] are raised and lowered with $\eta_{\mu\nu} = \mathrm{diag}(1,-1)$, and where

$$
\begin{aligned}
f_{\mu\nu} &= \partial_\mu a_\nu - \partial_\nu a_\mu \qquad (16)\\
\chi &= \alpha + \imath\beta \qquad (17)\\
\phi &= \mu + \imath\nu \qquad (18)\\
D_\mu\chi &= (\partial_\mu - \imath\, a_\mu)\chi \qquad (19)\\
D_\mu\phi &= (\partial_\mu - \frac{\imath}{2}\, a_\mu)\phi\ . \qquad (20)
\end{aligned}
$$

The reduced action, Eq. 15, is invariant under the gauge transformation

$$
\begin{aligned}
a_\mu &\quad \to a_\mu + \partial_\mu\Omega \qquad (21)\\
\chi &\quad \to e^{\imath\Omega}\chi\ , \qquad (22)\\
\phi &\quad \to e^{\imath\Omega/2}\phi \qquad (23)
\end{aligned}
$$

which corresponds to the residual $U(1)$ gauge invariance of Eqs. 12-14. From Eqs. 15-22, we see that the spherical *Ansatz* effectively yields a system very similar to the Abelian Higgs model considered above. In this reduced system the variables $a_0(r,t)$ and $a_1(r,t)$ play the role of the gauge field, whereas the variables $\chi(r,t)$, which parameterizes the residual components of the 4-dimensional gauge field, and $\phi(r,t)$, which parameterizes the 4-dimensional Higgs field, both behave as 2-dimensional Higgs fields. Of course, the presence of metric factors (powers of r) in the action Eq. 15 is a reminder that we are really dealing with a 4-dimensional system.

Regularity of the 4-dimensional field configuration for $r = 0$ requires

$$\begin{aligned} &\chi(r=0) = -\imath \\ &\mathrm{Im}\phi(r=0) = 0 \ . \end{aligned} \tag{24}$$

Although one could modify these boundary conditions by a singular gauge transformation, this would introduce unnecessary complications. So we will impose Eqs. 24, in addition to some other boundary conditions that also follow from the regularity of the 4-dimensional configuration. It is also worth noting here that non-singular gauge transformations satisfy the condition that the gauge function $\Omega(r,t)$ vanishes at $r = 0$ (or is a multiple of 2π).

We shall work in the $a_0 = 0$ (or $A_0 = 0$) gauge throughout. In the overlaying 4-dimensional theory, if one compactifies 3-space to S^3 by identifying the points at infinity, it is well known that the vacua correspond to the topologically inequivalent ways that S^3 can be mapped into $SU(2) \sim S^3$[12]. These maps are characterized by the third homotopy group of $SU(2)$, and a vacuum can be labeled by an integer called the homotopy index or winding number. The effective 2-dimensional theory inherits a corresponding vacuum structure. From Eq. 15 it is apparent that the vacuum states are characterized by $|\chi| = |\phi| = 1$, with the additional constraint that $\imath\chi^*\phi^2 = -1$ (as well as $D_1\chi = D_1\phi = 0$). A convenient zero-winding vacuum is given by $\chi_{vac} = -\imath$, $\phi_{vac} = 1$. Nontrivial vacua can be obtained from this vacuum via gauge transformations in which the gauge function $\Omega \to 2\pi n$ (for non-zero integers n) as $r \to \infty$. Note that the compactification of 3-space ensures that at infinity Ω is a multiple of 2π. Since Ω has been locked down to zero at $r = 0$, the winding of such a gauge transformed configuration is just the integer n. For example, a typical winding-number one vacuum obtained from the previous trivial vacuum is given by $\chi_{vac} = -\imath\exp[\imath\theta(r)]$, $\phi_{vac} = \exp[\imath\theta(r)/2]$ and $a_{1\,vac} = \partial_r\theta(r)$, where $\theta(r)$ varies from 0 to 2π as r changes from 0 to ∞. By taking advantage of the freedom of performing a time independent gauge transformation, however, one can also choose a gauge where $\chi(r)$ and $\phi(r)$ tend to values different from $-\imath$ and 1 as $r \to \infty$ (the condition $\imath\chi^*\phi^2 \to -1$ must be preserved). Indeed, it will be convenient to choose one such gauge to parameterize the sphaleron.

In making a topological transition between two inequivalent vacua, one must leave the manifold of vacuum configurations and pass over an energy barrier. Along such a trajectory there will be a configuration of maximum energy. Of all these

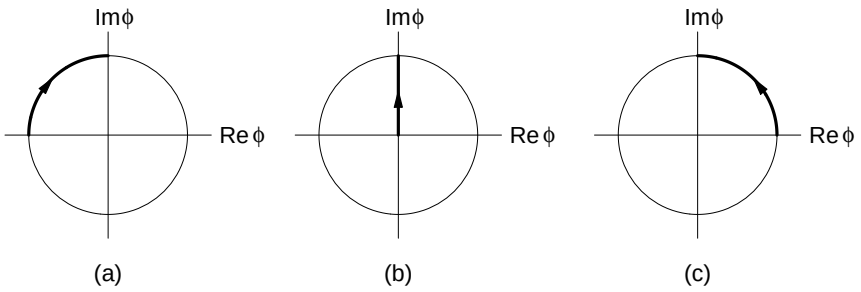

Figure 4: The behavior of the ϕ field for a typical topological transition. The χ field has a behavior similar to the one in Fig. 2.

maximal energy configurations, the sphaleron has the lowest energy and represents a saddle point along the energy ridge separating inequivalent vacua[2]. The sphaleron can be expressed in the spherical *Ansatz*, and it is convenient to choose a gauge in which $a_\mu = 0$ and

$$\begin{aligned} \chi_{sph}(r) &= \imath[2f(r) - 1] \\ \phi_{sph}(r) &= \imath h(r) \ , \end{aligned} \tag{25}$$

where f and h vary between 0 and 1 as r changes from 0 to ∞ and are chosen to minimize the energy functional.

This choice of gauge for the sphaleron is slightly peculiar in the following sense. Finite energy configurations, like Eq. 25, asymptote to pure gauge at spatial infinity. Typically a gauge is chosen so that the appropriate gauge function is unity at spatial infinity, and then space can be compactified to the 3-sphere. But consider the spherical gauge function Eq. 14 with $\Omega(r)$ independent of time and varying from 0 to π as r goes from 0 to ∞. From Eqs. 22-23 we see that the corresponding $\chi, \phi \to \imath$ for large r, which is the same as the sphaleron boundary conditions at spatial infinity. Note, however, that $U \mid_{r\to\infty} = \imath\boldsymbol{\sigma} \cdot \hat{\mathbf{x}}$ is direction dependent, so space cannot be compactified. An arbitrary element of $SU(2)$ can be parameterized by $\mathrm{b}_0\mathbf{1} + \imath\boldsymbol{\sigma} \cdot \mathbf{b}$ where $\mathbf{1}$ is the two by two unit matrix and $\mathrm{b}_0^2 + \mathbf{b}^2 = 1$. Hence $SU(2) \sim S^3$, and defining the north and south poles by $\pm\mathbf{1}$, we see that $\imath\boldsymbol{\sigma} \cdot \mathbf{b}$ with $\mathbf{b}^2 = 1$ parameterizes the equatorial sphere. Thus, the sphere at infinity is mapped onto the equatorial sphere of $SU(2)$. In this gauge, a topology changing transition proceeding over the sphaleron corresponds to a transition where the fields wind over the lower hemisphere of $SU(2)$ before the transition and over the upper hemisphere after the transition, with a net change in winding number still equal to one. In this gauge, the behavior of the χ field in a topological transition will be very similar to the behavior of the Higgs field in the 2-dimensional model, already illustrated in Fig. 2. The behavior of the ϕ field is illustrated in Fig. 4. We could of course work in a compactified gauge where a topological transition would occur between a field with no winding and a field with unit winding, as in Fig. 1, but the sphaleron would look more complicated. The

Figure 5: Behavior of the χ field in a topology changing transition. The various shades of gray code the phase of the complex field. The field starts as an excitation about the trivial vacuum, passes over the sphaleron and then emerges as an excitation about the vacuum of unit winding. Note the persistent strip of 2π phase change after the wave bounces off the origin.

advantage of Eq. 25 from a computational perspective is that perturbations about the sphaleron can be more easily parameterized.

In the sphaleron configuration the χ field has a zero at some non-zero value of r, whereas the ϕ field has a zero for $r = 0$ corresponding to the vanishing at the origin of the actual 4-dimensional Higgs field. The zero of χ is reminiscent of the zero which characterizes the sphaleron of the Abelian Higgs model. However, as shown in Ref. [13], it is the zero of the true Higgs field (i.e. the zero of ϕ) which carries a deeper significance and should be associated with the actual occurrence of the topological transition. Nevertheless, since the phase changes of χ are more dramatic than those of ϕ, for purposes of illustration it is often more convenient to plot χ. Figure 5 illustrates a typical topological transition. The configuration starts as a small excitation about the trivial vacuum defined above, passes over the sphaleron and then emerges as a configuration that undergoes a 2π phase change.

3 Numerical study of classically allowed processes

For energy larger than the sphaleron energy E_{sph}, i.e. for $\epsilon > \epsilon_{sph} = g^2 E_{sph}$, classical evolution which changes the topology of the fields becomes possible. Solutions to the classical equations of motion provide the dominant contributions in a weak coupling expansion of the path integrals describing transition processes between coherent states. The existence of topology-changing solutions indicates that the cor-

responding processes, which because of the change of topology violate baryon number, are not suppressed. However it would be premature to conclude that baryon number violation can occur with non-negligible amplitude in high energy collisions. Indeed, the number of particles in the initial state of such processes is small and, in terms of the rescaled fields used in the description of the classical evolution, this converts into a rescaled particle number $\nu = g^2 N$ which tends to zero as $g \to 0$. Thus, in order to establish evidence for baryon number non-conservation in high energy collisions, one must show that topology changing classical evolution can occur with arbitrarily small ν in the initial state.

The primary impediment for rapid baryon number violation seems to be a phase space mismatch between initial states of low multiplicity and final states of many particles. The authors of Ref. [14] look at simplified models and observe that, classically, it is difficult to transfer energy from a small number of hard modes to a large number of soft modes. However, Ref. [15] finds that for pure Yang-Mills theory in 2-dimensions the momenta can be dramatically redistributed, but unfortunately the initial particle number seems to be rather large in their domain of applicability. It is the purpose of our investigation to shed light on the situation in 4-dimensions when the Higgs field is added.

Given any classical evolution, because of the dispersion of the energy, the fields will asymptotically approach vacuum values. Thus, for times $t < -T_i$ and $t > T_f$ and sufficiently large T_i, T_f, the equations of motion will reduce to linearized equations describing the small oscillations of the system about a vacuum configuration. In this linear regime, the evolution of the fields will be given by a superposition of independent harmonic oscillators (the normal modes). In terms of the frequencies ω_n and amplitudes a_n of these oscillators the (rescaled) energy and particle number are given by

$$\epsilon = \sum_n \omega_n a_n^* a_n \tag{26}$$

and

$$\nu = \sum_n a_n^* a_n. \tag{27}$$

Thus for any classical evolution the energy ϵ and the particle numbers ν_i and ν_f of the asymptotic initial and final states are well defined. (The energy is of course conserved and well defined even in the non-linear regime.) In addition, because of the fact that the fields approach vacuum values for $t \to \pm\infty$, the winding numbers of initial and final configuration are also well defined. Because of the sphaleron barrier, the energy ϵ of all the classical solutions with a net change of winding number is bounded below by the sphaleron energy ϵ_{sph}. The problem one would like to solve, then, is whether the initial particle number ν_i of these solutions can be arbitrarily small, or more generally, one would like to map the region spanned by all possible values of ϵ and ν_i for the topology changing classical evolution. The highly non-linear nature of the equations of motion makes an analytic solution unlikely, even if one is

willing to make the crudest approximations. The problem is however amenable to solution by computational techniques. In this section we will illustrate the strategy we have followed to formulate it on the computer and the progress we have been able to make towards its solution.

The fundamental computational ingredient consists in the implementation of a numerical solution of the equations of motion. We start from the Hamiltonian formulation of the equations of motion for the continuum system in the $a_0 = 0$ gauge. In such a formulation the variables

$$a_1(r), \quad \chi(r), \quad \phi(r) \tag{28}$$

form a set of canonical coordinates, conjugate to the momenta

$$\begin{aligned} E(r) = &\quad r^2 \partial_0 a_1, \\ \pi_\chi(r) = &\quad \partial_0 \chi, \\ \pi_\phi(r) = &\quad r^2 \partial_0 \phi \ . \end{aligned} \tag{29}$$

The evolution of these variables is generated by the Hamiltonian

$$\begin{aligned} H = \int_0^\infty dr \qquad & \Big[\frac{E^2}{2r^2} + |\pi_\chi|^2 + \frac{|\pi_\phi|^2}{r^2} + |D_r \chi|^2 + r^2 |D_r \phi|^2 \\ & + \frac{1}{2r^2} \Big(\ |\chi|^2 - 1 \Big)^2 + \frac{1}{2}(|\chi|^2 + 1)|\phi|^2 + \mathrm{Re}(i \chi^* \phi^2) \\ & + \lambda \, r^2 \ \Big(|\phi|^2 - 1 \Big)^2 \ \Big] \ . \end{aligned} \tag{30}$$

Gauss' law

$$\partial_r E = \imath (\pi_\chi^* \chi - \chi^* \pi_\chi) + \imath (\pi_\phi^* \phi - \phi^* \pi_\phi) \tag{31}$$

expresses the residual invariance of the system under time independent local gauge transformations and is imposed as a condition on the initial state. It is then automatically conserved by the equations of motion.

To solve the equations of motion numerically the system must be discretized. It is convenient to use the formalism of lattice gauge theories. The r-axis is subdivided into N equal subintervals of length Δr with finite length $L = N \, \Delta r$. Thus, the lattice sites have spatial coordinates $r_i = i \Delta r$ with $i = 0 \cdots N$, and the midpoints between lattice sites have coordinates $r_{i+1/2} = (i + 1/2) \Delta r$ with $i = 0 \cdots N - 1$. The fields χ, ϕ, π_χ and π_ϕ are then represented by discrete variables defined over the end points of the intervals, $\chi_i = \chi(r_i)$, $\phi_i = \phi(r_i)$, etc.; whereas the fields a_1 and E are defined over the intervals themselves by $a_{1i} \equiv a_i = a_1(r_{i+1/2})$ and $E_i = E(r_{i+1/2})$ (for notational simplicity we have dropped the spatial subscript on the discretized gauge field). The covariant derivatives are then replaced by covariant finite differences, e.g.

$$D_r \chi \to \frac{\exp[-\imath a_i \, \Delta r] \, \chi_{i+1} - \chi_i}{\Delta r} \qquad i = 0 \cdots N - 1 \ , \tag{32}$$

and like the gauge fields they are to be thought of as living on the links between lattice sites. The rest of the discretization is straightforward. One obtains a discretized Hamiltonian H_D expressed in terms of a finite set of variables, which still possesses exact local gauge invariance under the transformations of Eqs. 21-22 provided that $a_1 \to a_1 + \partial_r \Omega$ is replaced with the finite difference formula

$$a_i \to a_i + \frac{\Omega_{i+1} - \Omega_i}{\Delta r} \qquad i = 0 \cdots N-1 \ , \tag{33}$$

where $\Omega_i = \Omega(r_i)$. From H_D one can easily obtain the canonical evolution equations for the discretized variables. Gauss' law, which now takes a discretized form, must be imposed on the initial state and is then preserved (exactly) by the time evolution because of the gauge invariance of the discretized system. In practice we have used values of N equal to 256, 512 and 1024 and values of Δr equal to 0.2, 0.1 and 0.05 in respectively study the properties of the system (with $\lambda = 0.1$). We found these parameters to be adequate for obtaining, on the one hand, a reasonable approximation to the continuum system and, on the other, a cut-off on r sufficiently large to allow for an effective linearization of the equations of motion before the waves hit the boundary. The restriction to uniform spacing of the subintervals on the r-axis is not fundamental and we have also implemented a discretization where Δr increases as one moves out on the r-axis. In this manner one can effectively make the system larger and delay the effects of the impact of the waves with the boundary without worsening the spatial resolution near $r = 0$, where most of the non-linear dynamics takes place. We have found however that the advantages one gains hardly warrant the additional complications introduced by the non-uniform spacing.

For the numerical integration of the time evolution we have used the leap-frog algorithm. Since this algorithm, or the equivalent velocity Verlet algorithm, constitutes one of the fundamental techniques for the integration of ordinary differential equations of the Hamiltonian type and as such is textbook material, we will not discuss it in any great detail. Essentially, given conjugate canonical variables q_i and p_i which obey equations

$$\begin{aligned} \frac{dq_i}{dt} &= g_i(p), \\ \frac{dp_i}{dt} &= f_i(q), \end{aligned} \tag{34}$$

one evolves the values of q and p from some initial t to $t + \Delta t$ as follows. In a first step p_i is evolved to the mid-point of the time interval by

$$\begin{aligned} p_i \to p_i' = &\quad p_i + f_i(q)\frac{\Delta t}{2}, \\ q_i \to q_i' = &\quad q_i \ . \end{aligned} \tag{35}$$

(Although q_i is left unchanged, it is convenient to consider the step formally as a transformation of the entire set of canonical variables.) In a second step one evolves

the coordinates from their initial value $q_i = q_i'$ to their value at the end of the interval

$$\begin{aligned} p_i' \to p_i'' = &\quad p_i', \\ q_i' \to q_i'' = &\quad q_i' + g_i(p')\Delta t \ . \end{aligned} \tag{36}$$

Finally the momenta are evolved from their value at the midpoint to the final value

$$\begin{aligned} p_i'' \to p_i''' = &\quad p_i'' + f_i(q'')\frac{\Delta t}{2}, \\ q_i'' \to q_i''' = &\quad q_i'' \ . \end{aligned} \tag{37}$$

One can easily verify that these equations reproduce the correct continuum evolution from t to $t + \Delta t$ up to errors of order $(\Delta t)^3$. Moreover, the algorithm has the very nice property that all three steps above constitute canonical transformations and that it is reversible (in the sense that starting from q_i''', $-p_i'''$, up to numerical errors one would end up exactly with q_i, $-p_i$). Another very nice feature of the algorithm is that, although the evolution of the variables is affected by errors of order $(\Delta t)^3$, the energy of a harmonic oscillator, and therefore also of any system which can be decomposed into a linear superposition of harmonic oscillators, is conserved exactly (always up to numerical errors). In a sequence of several iterations of the algorithm after the momenta have been been evolved by the initial $\Delta t/2$, the first and third step can be combined into a single step whereby the momenta are evolved from the midpoint of one interval to the midpoint of the next one, "hopping over" the coordinates, which are evolved from endpoint to endpoint. This motivates the name assigned to the algorithm.

With a good grasp on the numerical solution of the equations of motion, we can now turn to the second crucial component of the computation, namely the identification of the particle number in the initial state. One could easily parameterize an initial configuration of the system consisting of incoming waves in the linear regime. However, it would be extremely difficult to adjust the parameters so as to insure that a change of winding number occurs in the course of the subsequent evolution. For this reason it is much better to parameterize the initial configuration of the system at the moment when a change of topology occurs. Thus our strategy consists in implementing a time-reversed solution of the equations of motion, where the initial configuration is the configuration of the system at the moment when it passes over the sphaleron barrier and the asymptotic configuration for large t will be interpreted as a time-reversed incoming state.

Topology changing transitions within the spherical ansatz are characterized by the vanishing of ϕ at $r = 0$ and the the vanishing of χ at nonzero r. For a sequence of configurations that pass directly through the sphaleron these two zeros occur at the same time. However, this is not the most general case and the zeros of ϕ and χ need not occur simultaneously [16]. So we have parameterized initial configurations in terms of coefficients c_n of some suitable expansion of the fields and their conjugate

momenta, constrained only by the fact that the field χ must have a zero at some finite r, as in the sphaleron configuration. Furthermore, we can use gauge invariance to make this field pure imaginary. The field ϕ is only restricted to obey the boundary conditions and does not necessarily vanish at the origin (although it will vanish at some point in its evolution). [a]

In practice, computational considerations will limit the number of parameters we will be able to use. We will then evolve the system until the dispersion of the energy brings it to the linear domain. At this point, we can calculate the amplitudes of the normal modes of oscillation and the particle number of the system in its asymptotic state. It is clear that every set of coefficients c_n will determine one definite value for the energy ϵ and particle number ν of the asymptotic state. In calculating the particle number, one should use only the lower lying modes since higher modes probe wave lengths of order the lattice spacing. For our lattice parameters, we found that considering the first 50 to 100 modes is reasonable. We should point out that an arbitrary initial configuration is not necessarily guaranteed to change topology. However, by evolving the configuration both forward and backward in time we can easily verify whether topology changes, and initial configurations that do not change the topology can be rejected. By reversing the time evolution, then, we will have defined an initial asymptotic configuration with energy ϵ and particle number ν, which in the course of its evolution undergoes a change of topology. By varying the values of the parameters c_n we will be able to study the properties of such field evolution and, in particular, explore the domain of permissible values for ϵ and ν. It should be obvious at this point that the determination of the normal mode amplitudes is another crucial ingredient of the computation.

The normal modes of oscillation can be calculated starting from the linearized equations of motion. These equations can be obtained from an expansion of the Hamiltonian up to second order in the deviation of fields from a vacuum configuration. For conciseness of presentation we will not reproduce here their explicit form, but will limit ourselves to a discussion of the general properties of the normal modes. The normal modes can be obtained by assuming an oscillatory evolution for the fields of the type

$$\begin{aligned} \delta\chi(r,t) = &\quad \chi^{(n)}(r)\sin[\omega_n t] \\ \pi_\chi(r,t) = &\quad \pi_\chi^{(n)}(r)\cos[\omega_n t]\ . \end{aligned} \tag{38}$$

In this equation we have made reference only to one pair of conjugate fields, but the equation should be complemented with a similar assumption for the pairs a_1 and E, $\delta\phi$ and π_ϕ, which are a priori all coupled together with $\delta\chi$ and π_χ in the equations of evolution. We have used the symbol δ to denote the deviations of the fields χ and ϕ from their vacuum values $\chi = -\imath$ and $\phi = 1$. All of the other fields vanish in the

[a] Of course we could equally well arrange ϕ to be pure imaginary and to vanish at the origin, with no restriction χ on other than its boundary conditions.

trivial vacuum configuration. For the discretized system, r should be replaced by an index i.

Substituting the *Ansatz* of Eqs. 38 into the equations of motion one obtains a set of eigenvalue equations. Their solution determines the possible values of ω_n as well as the corresponding eigenfunctions (or more properly eigenvectors in the discretized case) $\delta\chi^{(n)}(r)$, $\pi_\chi^{(n)}(r)$ etc. We have determined eigenvalues and eigenfunctions both numerically, for the discretized system, and analytically, for the continuum system. One finds that the normal modes of oscillations are naturally grouped together into four sets of modes:

i) a set of modes where only the imaginary part of the fields $\delta\chi$ and π_χ is non-vanishing. These correspond to an oscillation of the modulus of the χ field .

ii) a set of modes where only the real part of the fields $\delta\phi$ and π_ϕ is non-vanishing. These correspond to an oscillation of the modulus of the ϕ field .

iii) and iv) two sets of modes where the real part of $\delta\chi$, π_χ, the imaginary part of $\delta\phi$, π_ϕ as well as a_1 and E are coupled together and non-vanishing. These correspond to oscillations of the phases of χ and ϕ (in coherence or opposition of phase), accompanied corresponding oscillations of the gauge fields.

Given the expressions for the eigenfunctions it is possible to extract the amplitudes of the normal modes of oscillation $a_n(t)$ by taking suitable convolutions of the eigenfunctions with the fields and momenta. This procedure exploits various properties of orthogonality which the eigenfunctions satisfy. One subtle point, however, involves the need to fix the gauge. The normal modes are obtained on the basis of an expansion into small oscillations around the trivial vacuum configuration with constant fields (one could of course expand around any fixed vacuum configuration, but the formulae are much simpler if one expands around constant fields). However there is no guarantee that the evolution of the fields will lead to an asymptotic regime of small fluctuations precisely around such a vacuum configuration. Indeed, in general this will not happen and the actual configuration will typically differ from the one used to derive the normal modes by a large gauge transformation. The remedy is easy enough. One can perform a gauge transformation to a fixed gauge which differs at most by small fluctuations from the one where the expansion has been performed. In our computations we have used the unitary gauge defined by $\mathrm{Arg}\chi(r) = -\pi/2$, transforming the fields to this gauge at some definite time t_0, at which point the appropriate amplitudes may be extracted. At subsequent times the fields might no longer be small perturbations about the trivial vacuum, so every time the amplitudes are calculated we first enter the above gauge. An alternative approach, which we have also implemented, consists in deriving the linearized equations of motion for a complete set of gauge invariant quantities [16](we have used $|\chi| - 1$, $|\phi| - 1$, the electric field E, the difference of phases $\mathrm{Arg}\chi - 2\mathrm{Arg}\phi$ and the time derivatives of all these quantities). Following a procedure similar to the one outlined above (cf. Eq. 38) one can derive the eigenvalues and eigenfunctions for the small oscillations of these quantities (the eigenvalues are identical, of course, to those obtained using

Figure 6: Sphaleron decay in the four dimensional $SU(2)$ Higgs model: evolution of the χ field. The values of the phase of the complex field are coded by different shades of gray. When the evolution reaches the linear regime, a gauge transformation, indicated by the sudden change of shading, is performed to extract the normal mode amplitudes.

gauge variant quantities) and extract the amplitudes through suitable convolutions with the evolving fields. We have verified that the two procedures produce identical results.

We can now turn our attention to the figures that illustrate our results for a system with coupling constant $\lambda = 0.1$. Figure 6 illustrates the behavior of the field χ following the decay of the sphaleron after a slight initial perturbation. We have found it very convenient and informative to use color to code the phase of the complex fields. Unfortunately the illustrations in these pages cannot be reproduced in color and we have tried to render the variation of the phase with a gray scale. From Fig. 6 it is clear that the energy, which is concentrated in the neighborhood of $r = 0$ in the sphaleron configuration, disperses and gives rise to a pattern of outgoing waves. The sudden variation of tonality at some point in the time evolution indicates the change of phase induced by the gauge transformation to the unitary gauge. In Fig. 7 we display the behavior of the particle number in the four normal modes of oscillations as function of time. It is apparent that, after an initial transition period where the particle number is not well defined, the quantities settle to values which are reasonably constant in time. We take this as evidence that the system has reached an asymptotic regime where one can meaniningfully define a conserved particle number. Finally, the evolution of the system can be time reversed, as we have discussed above, and the (time-reversed) final configuration can be considered as an asymptotic initial configuration with definite energy and particle number. The previously shown Fig. 5 illustrates the evolution

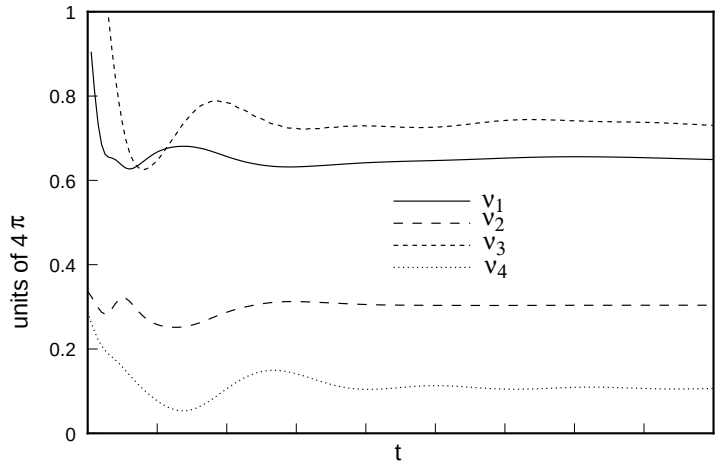

Figure 7: Sphaleron decay in the four dimensional $SU(2)$ Higgs model: behavior of the particle number in the four normal modes of oscillation of the linearized system as function of time. The sum in Eq. 27 extends over the first 50 modes for each of the four mode types.

obtained taking one such asymptotic initial configuration. The incoming waves are seen to merge in the neighborhood of the origin, where a change of topology takes place. The fact that the winding number of the field configuration has changed is indicated by the strip of rapidly varying tonality which persists in the neighborhood of the origin and codes the variation of the phase of χ. With color, this strip would appear as a vivid rainbow, left over as a marker of the change of topology of the evolving fields.

The configuration which sits on top of the sphaleron barrier can be parameterized by expanding into suitable components a complete set of independent fields. We have chosen these fields to be the perturbations $\Delta\chi$ and $\Delta\phi$ (not necessarily small) of the χ, ϕ fields of the sphaleron, the field a_1 and the momenta π_χ, π_ϕ. We avoid a redundant gauge degree of freedom by taking $\Delta\chi$ purely imaginary (like the χ field of the sphaleron itself). The final field needed to specify the initial configuration, i.e. the electric field E, can then be derived from Gauss law. We have parameterized these fields in terms of Bessel functions, chosen in such a way to respect appropriate boundary conditions at $r = 0$ and $r = L$. The coefficients c_n of the expansion can now be varied and, in this way, one can explore the region in the ϵ-ν plane spanned by all of the topology changing classical solutions.

Of course, the space of topology changing configurations is infinite and a random exploration of such space would not lead to very useful results. We must keep in mind that the interesting question is whether there is a lower bound in ν or, more generally, what is the lower boundary of the region spanned by all topology changing solutions in the ϵ-ν plane. This question can be investigated by methods of stochastic sampling. One can perform random small steps in the space of all configurations by varying the

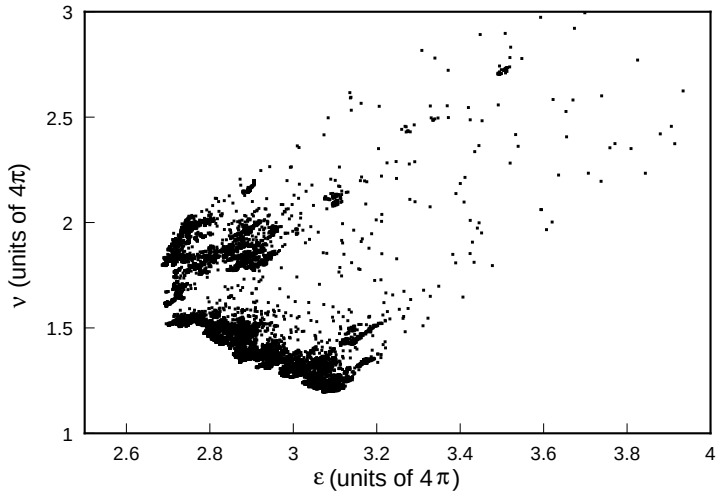

Figure 8: Monte Carlo results with lattice parameters of $\Delta r = 0.2$, $N = 256$ and L=51.2 and Higgs coupling $\lambda = 0.1$.

parameters c_n stochastically. After each change the new configuration is evolved until one can extract the particle number in the linear regime. Then the variations of energy and particle number $\Delta\epsilon$ and $\Delta\nu$ induced by the change Δc_n become well defined. A standard Metropolis Monte Carlo sampling technique consists in accepting or rejecting the change according to the value of the quantity $\Delta F = \beta\Delta\epsilon + \mu\Delta\nu$, where β and μ are parameters that weight what region of the ϵ-ν plane is explored. To be more precise, the change is accepted with conditional probability $P = \mathrm{Min}[1, \exp(-\Delta F)]$, which has the effect of producing configurations distributed according to a measure proportional to $\exp(-\beta\epsilon - \mu\nu)$. The parameters β and μ play the role of inverse temperature and chemical potential. By choosing these parameters appropriately one can drive the sampling towards low values of energy and particle number and thus explore the interesting region in the ϵ-ν plane. We have begun implementing this procedure and Fig. 8 illustrates our first results. It is interesting to note that the decay of a (slightly perturbed) sphaleron gives rise to a particle number $\nu \approx 1.9(4\pi)$. For $g = 0.6$ this corresponds to $N \approx 66$ physical particles. From Fig. 8 one can see that our sampling procedure has produced configurations with comparable energy and much smaller particle number. Of course the ultraviolet cutoff induced by the lattice discretization puts a lower limit on the ratio ν/ϵ, which occurs when only the highest mode is excited. We have used lattice parameters $\Delta r = 0.2$, $N = 256$ with $L = 51.2$ and have considered only the first 50 modes for each of the four types of normal modes. Hence the minimum value of ν/ϵ is of order $1/\omega_{max} \sim L/n_{max}\pi \sim 0.3$. Given our lattice resolution, we have saturated the lowest bound in particle number that we are sensitive to. This may be an indication that there is no lower bound on ν, but our calculation is still at a very preliminary stage and much more work will be needed to establish reliable results.

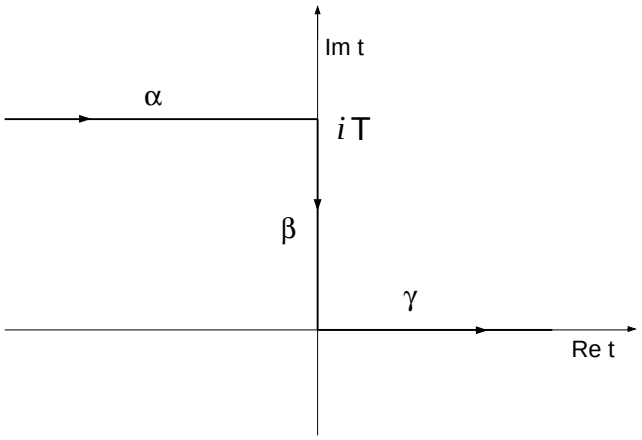

Figure 9: Complex time contour.

4 High energy baryon number violating processes below the sphaleron barrier

In the work of Ref. [7] Rubakov, Son and Tinyakov relate the probability of a topology changing process from a coherent state to the action of a complexified classical evolution along a special contour in the complex time plane. As shown in Fig. 9, this contour consists of a semiaxis parallel to the real axis $\alpha = (-\infty + \imath T \longrightarrow \imath T)$, followed by a segment $\beta = (\imath T \longrightarrow 0)$ of length T along the imaginary axis, followed by the real positive semiaxis $\gamma = (0 \longrightarrow +\infty)$. The word "complexified classical evolution" refers to the fact that the equations of motion must be analytically continued to complex fields. This has to be handled with some care for the case in which fields, such as $\chi(r)$ and $\phi(r)$, are already complex to begin with. In this case $\chi(r)$ and its complex conjugate, which we will denote here by $\bar{\chi}(r)$, must be considered as formally independent variables, which can be analytically continued separately, and do not necessarily satisfy the "reality condition" $\bar{\chi}(r) = \chi(r)^*$. The same applies to $\phi(r)$ and $\bar{\phi}(r)$.

The boundary conditions are of special importance. The solution must be real, in the sense specified above, along γ, where the asymptotic fields for $t \to +\infty$ represent the final state. The condition on the particle number in the initial state translates instead into the requirement that for very early times in the evolution (i.e. asymptotically for $t \to -\infty + \imath T$ along α) the fields must reduce to a superposition of normal modes of oscillation with amplitudes satisfying the equation

$$\bar{a}(-k) = e^{\theta} a^*(k) \tag{39}$$

where k is an index characterizing the radial momentum of the waves, and θ plays

the role of a chemical potential conjugate to the particle number in the initial state. It is clear from Eq. 39 that for $\theta \neq 0$ the fields cannot be real along α.

Computationally, it is convenient to think again of a time reversed evolution by which, starting from an initial configuration at $t = 0$ the fields undergo a Euclidean evolution along the imaginary time axis to $t = \imath T$ (i.e. following the oriented segment $-\beta$) and then a Minkowski evolution (along $-\alpha$) from $\imath T$ to $-\infty + \imath T$. For $t = 0$ for an x-axis discretized with N sites we have as free variables N real values of the field and N pure imaginary values of the conjugate momentum per each independent canonically conjugate field-momentum pair. The conditions that the normal mode amplitudes must satisfy Eq. 39 amount to N complex equations, i.e. $2N$ real equations again for each canonically conjugate field-momentum pair. Thus, in principle, one could evolve the fields from an initial *Ansatz* at $t = 0$ and adjust the initial variables so that Eq. 39 is satisfied. In practice, since the evolution equations along the imaginary time axis are elliptic, one cannot perform a forward integration. Rather, one must resort to some relaxation procedure or other global algorithm, by which one solves the evolution equations as a set of simultaneous non-linear equations for all points of a space-time grid. The situation is further complicated by the fact that, with complexified fields, one cannot just minimize a Euclidean action integral. We have developed a "second order" formulation, by which we minimize a constraint functional obtained from the modulus squared of the functions that must vanish at all grid points (an earlier part of this study was done in collaboration with Timothy Vaughan). In this case also we have used the formalism of lattice gauge theory to obtain a gauge invariant discretization. We tested our procedure in the context of the $2D$ Abelian Higgs model (one space, one time dimensions), where we found that it did reproduce the expected Euclidean solutions, including solutions with multiple bounces of the fields between two different topological sectors.

Another crucial component of the calculation consists in solving the evolution equations along the semiaxis $-\alpha$, from $\imath T$ to $-\infty + \imath T$ and extracting the normal mode amplitudes $a(k), \bar{a}(k)$. Here we feel that we have formalism and algorithm already in place, although we need to check that the integration remains stable with complexified fields.

In conclusion, the study of topology changing processes below the sphaleron barrier presents some additional challenges, the most notable being the need to integrate elliptic, rather than hyperbolic, equations over part of complex time path. The number of degrees of freedom and the complexity of the calculation, however, are not substantially different from those which characterize the numerical investigations of classically allowed processes, where, as we have shown above, the power of the computational tools are well adequate to produce interesting and accurate results. This warrants the expectation that even the classically forbidden processes will be amenable to a successful computational analysis.

Acknowledgments

This research was supported in part under DOE grant DE-FG02-91ER40676

and NSF grant ASC-940031. We wish to thank V. Rubakov for very interesting conversations which stimulated the investigation described here, A. Cohen, K. Rajagopal and P. Tinyakov for valuable discussions, and T. Vaughan for participating in an early stage of this work.

References

[1] G. 't Hooft, *Phys. Rev.* **D14** (1976) 3432.

[2] N. Manton, *Phys. Rev.* **D28** (1983) 2019;
F. Klinkhamer and N. Manton, *Phys. Rev.* **D30** (1984) 2212.

[3] A. Belavin, A. Polyakov, A. Schwarz and Yu. Tyupkin, *Phys. Lett.* **59B** (1975) 85.

[4] A. Ringwald, *Nucl. Phys.* **B330** (1990) 1.

[5] O. Espinosa, *Nucl. Phys.* **B343** (1990) 310.

[6] V. Kuzmin, V. Rubakov and M. Shaposhnikov, *Phys. Lett.* **B155** (1985) 36; see also P. Arnold and L. McLerran, *Phys. Rev.* **D36 (1987)** 581; L. Carson, X. Li, L. McLerran and R. T. Wang, *Phys. Rev.* **D42** (1990) 2127; D. Grigoriev, V. Rubakov and M. Shaposhnikov, *Phys. Lett.* **B216** (1989) 172; *Nucl. Phys.* **B342** (1990) 381; D. Grigoriev and V. Rubakov; ibid **B299** (1988) 67; M. Dine, O. Lechtenfeld and B.Sakita, *Nucl. Phys.* **B342** (1990) 381.

[7] V. Rubakov, D. Son and P. Tinyakov, *Phys. Lett.* **B287** (1992) 342.

[8] V. Rubakov and D. Son, *Nucl. Phys.* **B424** (1994) 55.

[9] P. Arnold and L. McLerran *Phys.Rev.* **D37** (1988) 1020.

[10] M. Hellmund and J. Kripfganz, *Nucl. Phys.* **B373** (1991) 749.

[11] B. Ratra and L. Yaffe, *Phys. Lett.* **B205** (1988) 57.

[12] R. Jackiw and C. Rebbi, *Phys. Rev. Lett.* **37** (1976) 172; C. Callan Jr., R. Dashen and D. Gross, *Phys. Lett.* bf 63B(1976) 334.

[13] E. Farhi, J. Goldstone, S. Gutmann, K. Rajagopal and R. Singleton Jr., BU-HEP-94-30 (1994).

[14] K. Rajagopal and N. Turok, *Nucl. Phys* **B375** (1992) 299; H. Goldberg, D. Nash and M. T. Vaughn, *Phys. Rev.* **D 46** (1992) 2585.

[15] C. Hu, S. Mathinyan, B. Müller, A. Trayanov, T. Gould, S. Hsu and E. Poppitz, DUKE-TH-95-85 (1995).

[16] E. Farhi , K. Rajagopal and R. Singleton Jr., BU-HEP-95-4 (1995).